Analytica Chimica Acta 1104 (2020) 156–163

Contents lists available at ScienceDirect

Analytica Chimica Acta

journal homepage: www.elsevier.com/locate/aca

Proximity-enabled bidirectional enzymatic repairing amplification for ultrasensitive fluorescence sensing of adenosine triphosphate

Shasha Li [a], Su Liu [b], Jingfeng Wang [a], Yihan Zhao [a], Rufeng Zhang [b], Xiaonan Qu [b], Yu Wang [a, *], Jiadong Huang [a, c], Jinghua Yu [c]

[a] College of Biological Sciences and Technology, University of Jinan, Jinan, 250022, PR China
[b] School of Water Conservancy and Environment, University of Jinan, Jinan, 250022, PR China
[c] Key Laboratory of Chemical Sensing & Analysis in Universities of Shandong, College of Chemistry and Chemical Engineering, University of Jinan, Jinan, 250022, PR China

HIGHLIGHTS

- It's the first time that palindromic fragment-mediated bidirectional enzymatic repairing amplification for ATP detection.
- Introduction of palindromic sequences can bypass the primers and avoid the inherent side reaction of the primer.
- The strategy showed excellent detection versatility for sensitively detecting a wide range of targets.
- This strategy shows promising potential in real sample analysis.

GRAPHICAL ABSTRACT

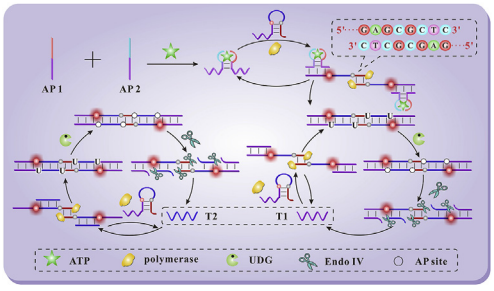

ARTICLE INFO

Article history:
Received 31 October 2019
Received in revised form
28 December 2019
Accepted 2 January 2020
Available online 3 January 2020

Keywords:
Adenosine triphosphate
Proximity ligation assay
Palindromic sequence
Bidirectional enzymatic repairing amplification
Fluorescence sensing

ABSTRACT

A novel fluorescence sensing strategy for ultrasensitive and highly specific detection of adenosine triphosphate (ATP) has been developed by the combination of the proximity ligation assay with bidirectional enzymatic repairing amplification (BERA). The strategy relies on proximity binding-triggered the release of palindromic tail that initiates bidirectional cyclic enzymatic repairing amplification reaction with the aid of polymerase and two DNA repairing enzymes, uracil-DNA glycosylase (UDG) and endonuclease IV (Endo IV). A fluorescence-quenched hairpin probe with a palindromic tail at the 3′ end is skillfully designed that functions as not only the recognition element, primer, and polymerization template for BERA but also the indicator for fluorescence signal output. On the basis of the amplification strategy, this biosensor displays excellent sensitivity and selectivity for ATP detection with an outstanding detection limit of 0.81 pM. Through simultaneously enhancing the target response signal value and reducing nonspecific background, this work deducted the background effect, and showed high sensitivity and reproducibility. Moreover, our biosensor also shows promising potential in real sample analysis. Therefore, the proximity-enabled BERA strategy indeed creates a simple and valuable fluorescence sensing platform for ATP identification and related disease diagnosis and biomedical research.

1. Introduction

Adenosine triphosphate (ATP), a major energy currency of the

* Corresponding author.
E-mail address: bio_wangy@ujn.edu.cn (Y. Wang).

https://doi.org/10.1016/j.aca.2020.01.006
0003-2670/

cell, plays a pivotal role in the regulation of cellular metabolism and biochemical pathways in cell physiology [1,2]. Aberrant expression of ATP is closely related to various diseases, for instance, malignant tumors, Alzheimer's disease, and Parkinson's diseases [3–5]. Plenty of evidences demonstrate that ATP has been acknowledged as a powerful and reliable indicator for the related diseases [6,7]. Accordingly, there is an urgent need for the development of rapid and sensitive strategies for ATP detection. The traditional methods for ATP identification are mainly based on high-performance liquid chromatography [8–10], mass spectrometry [11] and bioluminescence [12]. These methods, however, is complicated and technically demanding. Nowadays, various novel analytical methods, including chemiluminescence [13], electrochemiluminescence [14], surface-enhanced Raman scattering [15], electrochemistry [16], and colorimetry [17], have been extensively explored for ATP determination. Although these methods enable to detect ATP with high sensitivity, they might suffer from the shortcomings of time-consuming, expensive instrumentation, and poor reproducibility. Therefore, the development of more rapid, convenient, and sensitivity methods for ATP detection is still a grand challenge.

Recently, DNA nanotechnology has gained increasing interest because of its highly programmable nature, high precision, and ease of preparation [18]. As a result, various DNA-assisted assays, including the proximity ligation assay (PLA) [19–21], three-way junction [22], and the molecular pincer assay [23], have been designed. Among them, the proximity ligation assay, relying on the simultaneous recognition of target molecule by a pair of proximity probes, provides a promising way in accurate and quick detection of the target. Compared with conventional ATP assays, PLA-based biosensors are simpler and faster because they take the simplicity and variousness of DNA assembly to achieve one-step target detection [24,25]. However, the amplified signals tend to saturate easily, partly due to the depletion of substrates, and so this method is more suitable for analyzing targets of low abundance [26,27]. Thereby, a novel proximity-enabled bidirectional enzymatic repairing amplification (BERA) strategy was proposed for ultrasensitive and highly specific detection of the target. We designed a proximity hybridization-triggered signal switch by using a proximity complex to open a self-reporting molecular beacon (MB) with a palindromic tail at the 3′ end [28]. This switch could be used for a one-step fluorescence assay of different kinds of target biomolecules with corresponding affinity ligands. The enzymatic repairing amplification (ERA) [29,30] reaction was further coupled with this palindromic molecule switch by using polymerase for in situ recycling of the proximity complex. The strategy showed excellent detection versatility for sensitively detecting a wide range of targets such as oligonucleotides, proteins, or small molecules.

Palindromic sequence is a short inverted duplication nucleic acid fragment located in gene untranslated operon and specific protein binding region [31,32]. An interesting feature of palindromic sequence is the complementary strands being palindromic of each other. Such fascinating properties enable it to act as a primer in the field of nucleic acid molecular sensing. For instance, Li and co-authors devised a newly palindromic fragment-incorporated molecular beacon-based fluorescence aptasensor for genetic analysis of cancers [33] Zeng and co-authors presented an innovative and rationally engineered palindromic molecular beacon-based 'Z-scheme' photoelectrochemical biosensing protocol for the selective screening of kanamycin through DNA hybridization induced conformational conversion [34]. Shen and co-authors reported a highly sensitive and selective colorimetric assay based on a multifunctional molecular beacon with palindromic tail was proposed for the detection of target p53 gene [35]. Favorably, introduction of palindromic sequences can bypass the primers (namely, involving only single probe), and avoid the inherent side reaction of the primer, thus reducing the background signal and improving the detection sensitivity. To the best of our knowledge, regrettably, there is no study focusing on palindromic sequence-based signal-amplified strategy for ATP assay nowadays.

Herein, we develop a novel fluorescence sensing strategy based on proximity-enabled bidirectional enzymatic repairing amplification (BERA) for ultrasensitive and highly specific detection of ATP. In our assay, a fluorescence-quenched hairpin probe with a palindromic tail at the 3′ end (MB) is skillfully designed that functions as not only the primer for initiating BERA but also the indicator for fluorescence signal output. Introduction of palindromic sequences can effectively avoid the unwished extension attributed from the dynamic contact between the single-stranded primer with template, thus ultrahigh specificity of our strategy can be achieved for ATP detection. Additionally, the BERA reaction is initiated specifically by target ATP-aptamer binding and performed cyclically with the aid of polymerase and two DNA repairing enzymes, uracil-DNA glycosylase (UDG) and endonuclease IV (Endo IV) to produce amplified fluorescence signal [36–38]. On the basis of the combination of BERA with palindromic sequence, the nonspecific background can be suppressed. Therefore, this sensing strategy indeed create a versatile and convenient platform for ultrasensitive and highly specific detection of ATP and related disease analysis.

2. Experimental section

2.1. Materials and reagents

All oligonucleotides used in this research were purchased from Sangon Biotechnology Co. Ltd. (Shanghai, China) and were purified via HPLC. The detailed sequences of these oligonucleotides are listed in Table 1. Bst DNA polymerase (large fragment), *E. coli* uracil DNA glycosylase (UDG), endonuclease IV (Endo IV), adenosine triphosphate (ATP), guanosine triphosphate (GTP), cytidine triphosphate (CTP) and uridine triphosphate (UTP) were purchased from New England Biolabs (Beijing, China). dATP, dGTP, dCTP, dUTP, and dTTP were supplied by Takara Biotechnology Co. Ltd. (Dalian, China). The agarose and DNA marker were purchased by Takara Biotechnology Co. Ltd. (Dalian, China). All other chemicals were of analytical grade and were used without further purification. All solutions were prepared with ultrapure water that was obtained through a Millipore Milli-Q water purification system (Billerica, MA, USA) with an electric resistance >18 MΩ cm. The serum samples were collected from volunteers in compliance with all institutional and national guidelines.

The underlined bases in AP1 and AP2 are the split aptamer of ATP. Three functional regions in MB are marked in three different colors. Region I (purple) is the fragment complementary to the italics bases in AP1 and AP2. Region II (blue) is the secondary target-recognition region that can hybridize with secondary target gene. Region III (red) is a palindromic sequence. The molecular beacon (MB) is also chosen as signal probe by labeling with a pair of fluorophore (FAM) and quencher (Dabcyl).

2.2. Instruments

Gel electrophoresis was conducted using DYCZ-24DN electrophoresis cell (LIUYI, Beijing, China) and Bio-Rad Gel imaging system (Bio-Rad, USA). Fluorescence spectra were recorded using an Agilent Cary Eclipse spectrofluorometer (Agilent, USA) with excitation at 486 nm. The slit was set to be 5 nm for both the excitation and the emission.

Table 1
DNA oligonucleotides sequence used in this work.

Oligonucleotide name	Sequence (5' – 3 ') description
AP1	ACCTGGGGGAGTATGCAAGT*AGAACGAA*
AP2	*AGAGAGCGCC*TTGCTGCGGAGGAAGGT
MB	TTCGTTCTGCGCTCTCT (FAM)AGCCCTCCTTCTGTCCTTCTTCTTCCGT (Dabcyl)GAGAGCGCTC

2.3. Analytical protocol

The detailed procedure used to detect the target ATP was as follows: Firstly, AP1 (2.5 μL, 1 μM), AP2 (2.5 μL, 1 μM), MB (2 μL, 5 μM), Bst DNA polymerase (2 μL, 8 U μL^{-1}), UDG (2 μL, 1 U μL^{-1}), Endo IV (2 μL, 1 U μL^{-1}), 4 μL of 10 mM dNTPs (10 mM dATP, dGTP, dCTP, dUTP each), NEBuffer 2 (4 μL, 1 ×) and equal volumes of different concentrations of ATP (or ADP, GTP, CTP and UTP) were mixed and incubated at 50 °C for 90 min. Subsequently, the above mixed solution (40 μL) was mixed with 60 μL of ultrapure water and scanned using an Agilent Cary Eclipse spectrofluorometer in the wavelength range from 500 nm to 600 nm. And the fluorescent intensity at 519 nm was used for quantitative analysis. Unless noted otherwise, all experiments for ATP measurements were repeated three times in this study.

2.4. ATP assay in human serum samples

The healthy human serum samples were collected by centrifugation of whole blood after coagulation. Different concentrations of ATP (0, 10 pM, 100 pM and 1 nM) were separately spiked into the 10% diluted human serum samples and measured directly.

2.5. HPLC analysis for ATP detection

High performance liquid chromatography (HPLC) measurements were performed on an Agilent 1100 Series chromatograph equipped with a quaternary pump, a diode array detector (DAD), and an autosampler. An Allsphere ODS-C18 column (4.6 mm × 250.0 mm, 5 μm) from Waters was employed at room temperature (25 °C). The ATP standards and extracts were detected respectively through a gradient mobile phase of water and acetonitrile by a ratio of 40/60 (v/v). 1.0 mL min^{-1} was set as the flow rate. 20 μL of ATP sample was injected with 259 nm detection wavelength.

2.6. Polyacrylamide gel electrophoresis (PAGE) analysis

The 15% nondenaturating polyacrylamide gel electrophoresis (PAGE) was used in further confirm and characterize this amplification strategy. In the PAGE assay, the electrophoresis was performed in 1 × TBE buffer (50 mM Tris Borate, 2.0 mM EDTA, pH 8.2) at 110 V for 80 min. After staining by GelRed, the gel was visualized via fluorescence detection using a Bio-Rad Gel imaging system.

3. Results and discussion

3.1. Principle of the proposed BERA strategy for ATP assay

The working principle of the proposed fluorescence sensing strategy for ultrasensitive detection of ATP is illustrated in Scheme 1. The reaction system consists of six elements: two split aptamer fragment probes, AP1 and AP2, used for the recognition of target ATP, a fluorescence-quenched hairpin probe (MB) functioned as both the template and the primer for BERA and the indicator for fluorescence signal output, and three nucleic acid enzymes that are Bst DNA polymerase, uracil DNA glycosylase (UDG), and endonuclease IV (Endo IV), respectively. The split aptamer fragment probes contain two parts, split aptamer domains (pink and blue) acting as the target recognition components, and the split initiator regions (light purple) for BERA. The hairpin probe MB is comprised of three functional regions and two lesion incorporating sites. Region I (purple) is a nucleic acid segment complementary to the split initiator regions in AP1 and AP2. Region II (blue) is a specific secondary target recognition sequence that is the single stranded loop part of MB and can hybridize with secondary target gene. Region III (red) is a palindromic sequence that is locked in the initial state by the stem-loop structure. It is well-known that the palindromic sequences are able to hybridize with each other. In the presence of target ATP, the two split aptamer fragments can co-recognize ATP to form a stable AP1-ATP-AP2 structure, which can bring the two tail sequences into close proximity and bind to the 5′ terminus of MB that induces the conformation switch of MB. Immediately, the prelocked palindromic sequences within MB are released and intermolecular hybridization occurs. Accordingly, the bidirectional polymerization could be initiated with the aid of Bst DNA polymerase and four nucleotides dATP, dGTP, dCTP and dUTP, resulting in extended MB and MB duplex and accompanying by the release of the AP1-ATP-AP2 structure. It is worth noting that dUTP is used to instead of dTTP to incorporate lesions. So, four uracil (dU) nucleotides are incorporated in the extension product. Meanwhile, the four lesion sites are removed through cleaving the N-glycosidic bond between the uracil and the sugar, releasing the uracil base and forming the abasic sites (AP site). The AP site is then cleaved by Endo IV, which generates two new single-stranded DNA fragments T1 and T2. As much as AP1-ATP-AP2 structure behaviors, the liberated T1 and T2 can bind to other MBs respectively, promoting more rounds of bidirectional enzymatic repairing amplification reaction, thus numerous T1 and T2 are continuously produced. Eventually, more and more MB is opened, in which a remarkably enhanced fluorescence signal can be obtained due to the separation of fluorophore (FAM) from quencher (Dabcyl). Therefore, the proposed proximity-enabled BERA fluorescence sensing strategy indeed provides a rapid and versatile tool for ultrasensitive and highly specific detection of ATP.

3.2. Viability of the strategy for ATP assay

In order to confirm the feasibility of this strategy, a series of control experiments were investigated, and the results were depicted in Fig. 1. When the system was incubated with ATP, a significantly strong fluorescence signal was achieved with a emission peak at 519 nm (curve a). In contrast, it was found that a negligible fluorescent response was observed for the blank sample, implying a desirable signal-to-background ratio of 21.5 (curve b). This clearly revealed that the specific recognition of target ATP and the two split aptamer fragments can bring the two tail sequences into close proximity and activate MB-based bidirectional enzymatic repairing amplification. Thus numerous T1 and T2 were produced and more and more MB is opened, in which a remarkably enhanced fluorescence signal can be obtained. When the system was incubated with ATP in the absence of Bst DNA polymerase, there was a

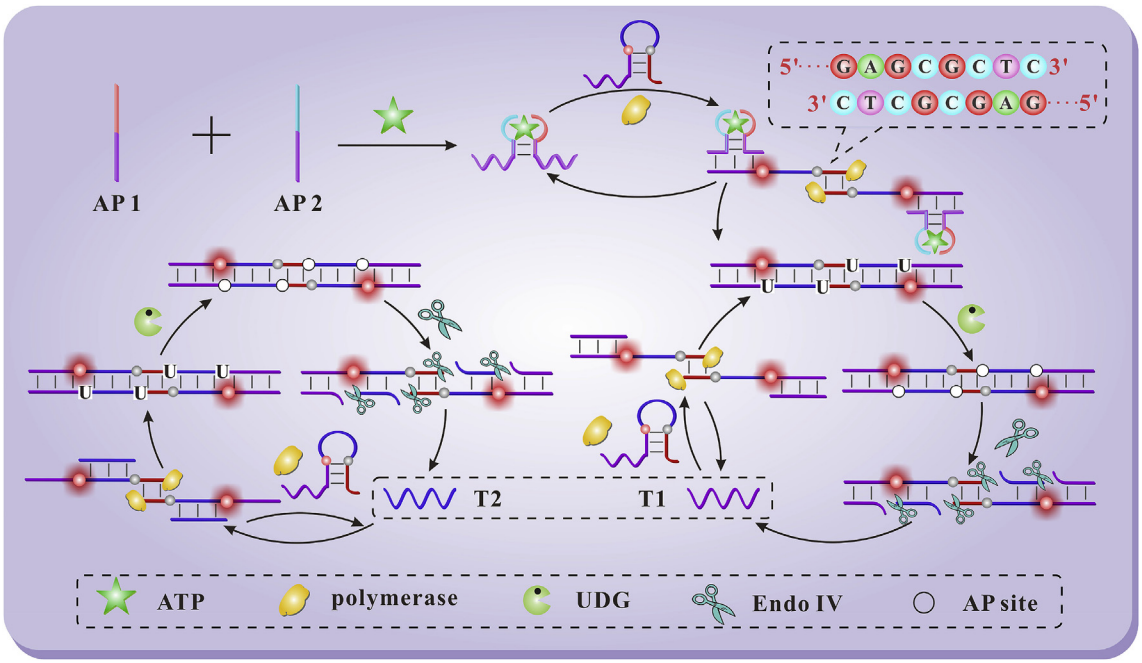

Scheme 1. Schematic illustration of fluorescent sensing of ATP based on proximity-enabled bidirectional enzymatic repairing amplification.

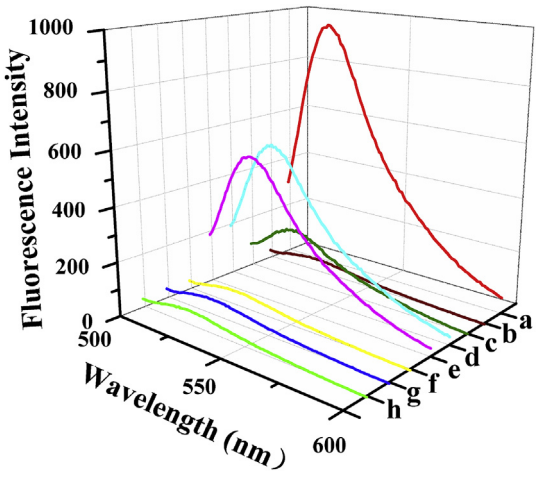

Fig. 1. Fluorescence emission spectra responses of the biosensor in the presence of 5.0×10^5 pM ATP (a), Curves b to h are for the control experiments which are performed with no target ATP (b), without Bst DNA polymerase (c), without UDG (d), without Endo IV (e), without Apt1 (f), without AP2 (g), and non-target ADP in place of ATP (h).

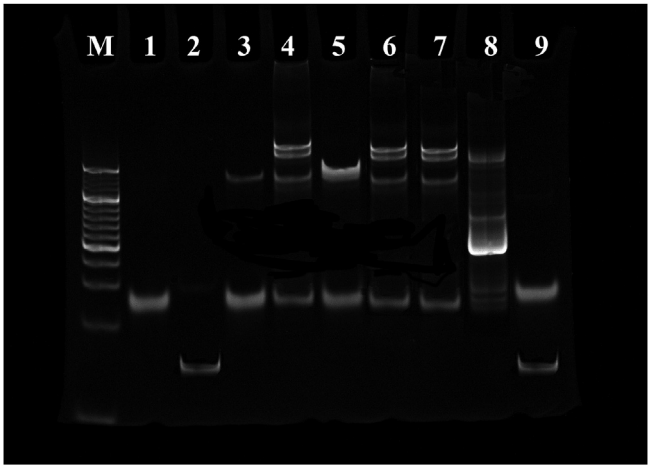

Fig. 2. Polyacrylamide gel electrophoresis characterization of the proposed strategy. Lane M, DNA marker; Lane 1, MB; Lane 2, AP1 and AP2 incubated with ATP; Lane 3, AP1, AP2, and MB incubated with ATP; Lane 4, AP1, AP2, MB, and Bst DNA polymerase incubated with ATP; Lane 5, AP1, AP2, MB, Endo IV, and UDG incubated with ATP; Lane 6, AP1, AP2, MB, Bst DNA polymerase, and Endo IV incubated with ATP; Lane 7, AP1, AP2, MB, Bst DNA polymerase, and UDG incubated with ATP; Lane 8, the positive sample; Lane 9, the blank sample.

weak fluorescence response, which demonstrated the bidirectional enzymatic repairing amplification reaction was initiated by Bst DNA polymerase-assisted extension reaction (curve c). When the system was incubated with ATP in the absence of UDG (curve d) or Endo IV (curve e) respectively, there are two moderate fluorescence signal was obtained, manifesting a certain amount of MB was opened due to the Bst DNA polymerase-assisted AP1-ATP-AP2 structure recycle amplification. In addition, two negligible fluorescence responses similar to that of the blank sample were observed in the absence of AP1 (curve f) or AP2 (curve g), which signified that the ATP-mediated assembly of two split aptamer fragments AP1 and AP2 was essential for the activation of fluorescence signal. Furthermore, when target ATP was replaced by non-target ADP, a dinky fluorescent signal was obtained, demonstrating the significantly increased fluorescence signal was triggered by the specific binding of target and aptamer (curve h). On the basis of these results, it was reasonably concluded that the proposed strategy held great potential for the quantitative assay of ATP with high specificity.

3.3. PAGE analysis

The polyacrylamide gel electrophoresis (PAGE) analysis was hired to directly proof of the reaction mechanism of the sensing system, and the results were displayed in Fig. 2. It was observed that the MB gave a bright band at Lane 1, illustrating no secondary

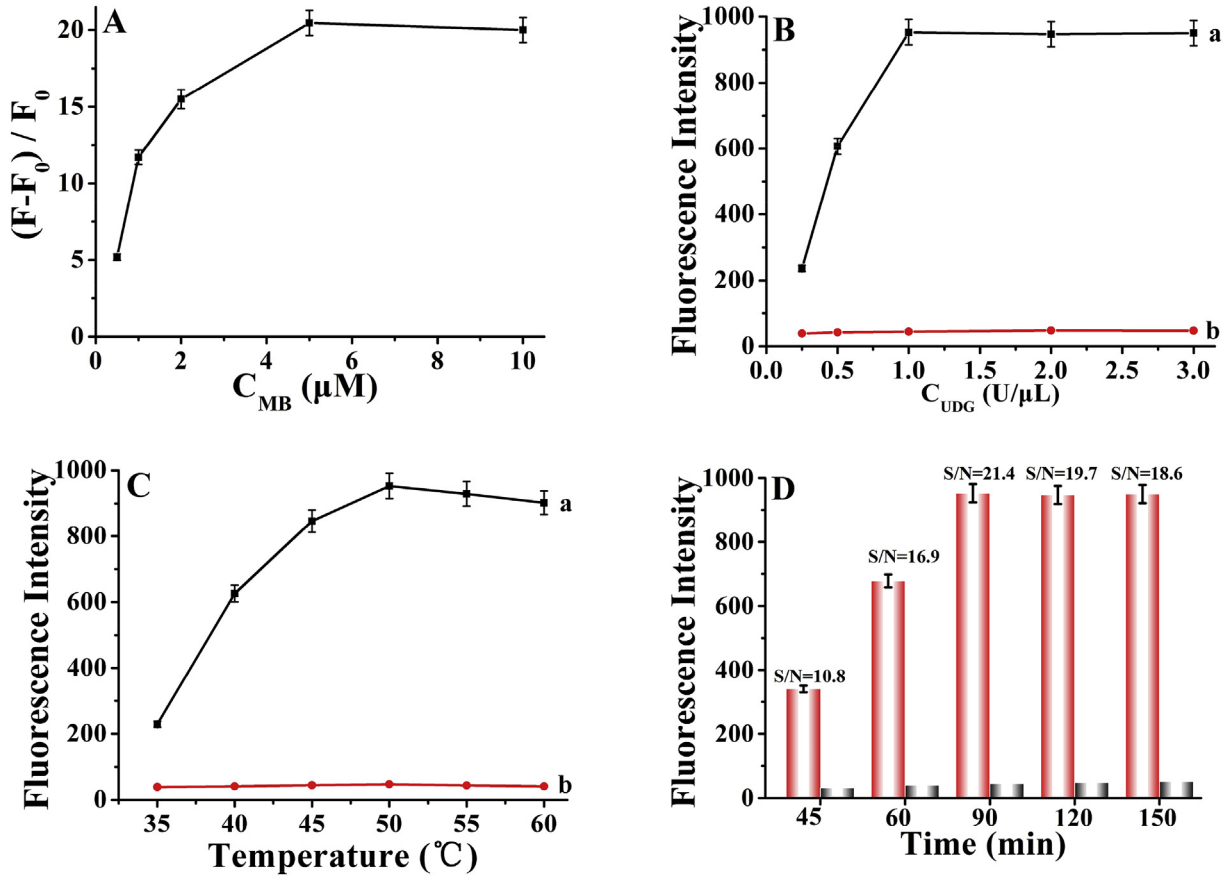

Fig. 3. (A) Effect of the concentration of MB on the $(F-F_0)/F_0$ value of the biosensor, F and F_0 represent the fluorescence signal intensity at 519 nm of the biosensor in the presence and absence of 5.0×10^5 pM ATP, respectively; (B) Effects of different concentrations of UDG on the fluorescence intensity at 519 nm of the biosensor in the presence (curve a) and absence (curve b) of 5.0×10^5 pM ATP; (C) Effect of the reaction temperature on the fluorescence intensity at 519 nm of the biosensor in the presence (curve a) and absence (curve b) of 5.0×10^5 pM ATP; (D) Effect of the reaction time on the fluorescence intensity at 519 nm of the biosensor in the presence (the red bar) and absence (the gray bar) of 5.0×10^5 pM ATP. Error bars are standard deviations across three repetitive experiments. (For interpretation of the references to color in this figure legend, the reader is referred to the Web version of this article.)

structure in the rationally designed DNA sequence. When incubated target ATP with two aptamer fragments AP1 and AP2, a new band appeared, suggesting AP1 and AP2 containing split ATP aptamer subunits could co-recognize ATP to form an AP1- ATP-AP2 structure (Lane 2). When incubated AP1, AP2, MB with ATP, a slim and weak band for the hybridized AP1-ATP-AP2/MB structures was observed at the top of Lane 3 in addition to those of excess MB probes. This indicated the specific recognition of ATP and two split aptamer fragments leads to the formation of AP1-ATP-AP2 structure that could bring the two tail sequences into close proximity and hybrid with the hairpin probe MB. When incubated AP1, AP2, MB, Bst DNA polymerase with ATP, we observed the brightness of

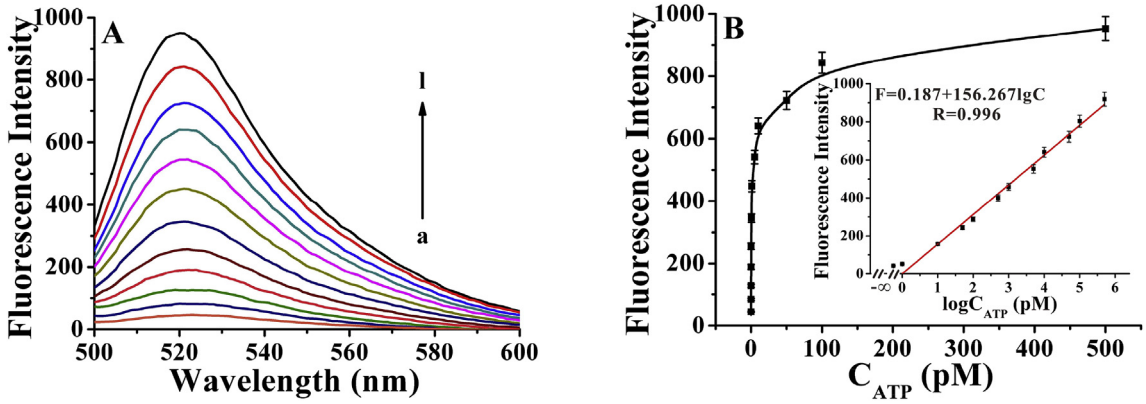

Fig. 4. (A) Fluorescence spectra responses of the biosensor to different concentrations of ATP (from curve a to l: 0, 1, 10, 50, 1.0×10^2, 5.0×10^2, 1.0×10^3, 5.0×10^3, 1.0×10^4, 5.0×10^4, 1.0×10^5, 5.0×10^5 pM); (B) The relationship of fluorescent signal intensities at 519 nm for different concentrations of ATP. Inset is the plot of the fluorescent intensity at 519 nm versus the logarithm value of ATP concentration. Error bars are standard deviations across three repetitive experiments.

Table 2
Comparison of different assay methods for the detection of ATP.

Detection methods	Detection range (pM)	Detection limit (pM)	Reference
Fluorescence	5.0×10^5–5.0×10^7	1.4×10^5	[39]
Electrochemistry	1.0×10^3–2.0×10^4	1.0×10^3	[40]
Chemiluminescence	2.0×10^3–8.0×10^4	1.4×10^3	[41]
Surface-enhanced Raman	1.2×10^1–2.0×10^3	1.2×10^1	[42]
Photoelectrochemical	1.0×10^4–1.0×10^6	3.2×10^3	[43]
Electrochemiluminescence	1.0×10^2–1.0×10^3	2.0×10^1	[44]
Fluorescence assay	1.0×10^0–5.0×10^5	0.81	This work

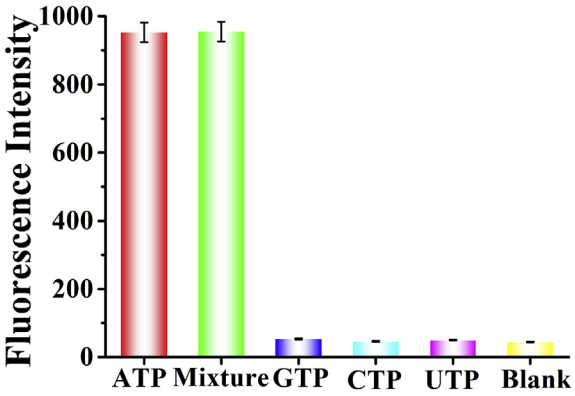

Fig. 5. The fluorescence responses at 519 nm obtained in response to different targets. The concentration of ATP was 500 nM and the concentration of non-target molecules was 500 nM. Error bars are standard deviations across three repetitive measurements.

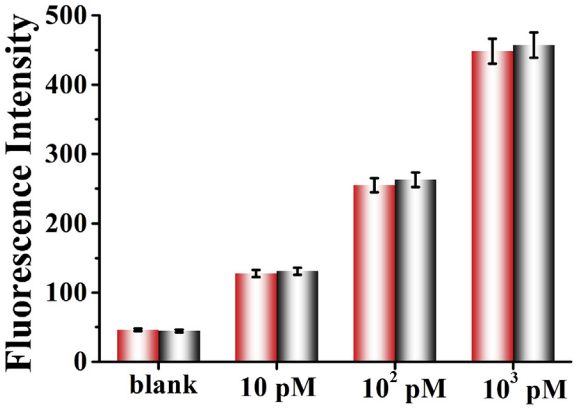

Fig. 6. The fluorescence responses of the biosensor for ATP detection in buffer (red bar) and serum samples (gray bar). The error bars are standard deviations across three repetitive experiments. (For interpretation of the references to color in this figure legend, the reader is referred to the Web version of this article.)

the band at the position of MB was visibly decreased compared to the corresponding bands of Lane 3, and a series of different molecular weight bands appeared (Lane 4), which may be attributed to the intra-/intermolecular polymerization products and/or intermediates. In addition, after incubation AP1, AP2, MB, UDG, Endo IV with ATP, the band similar to the Lane 3 was observed (Lane 5), it indicated that Bst DNA polymerase is essential for this reaction process. When the reaction system without UDG or Endo IV, bands appeared in Lane 6 and Lane 7 are similar to Lane 4, respectively, suggesting that the target-aptamer binding triggered BERA strategy was implemented owing to the perfect joint action by Bst DNA polymerase, UDG and Endo IV, lack of anyone, the work could not be completed. When incubated AP1, AP2, MB, Bst DNA polymerase, Endo IV, UDG with ATP, complicated and similar bands to Lane 4 could be found in Lanes 8, which was attributed to the synergistic effect of polymerase Endo IV and UDG. In contrast, for the blank sample, two wide bands, which are similar with Lane 1 and Lane 2, were observed on the Lane 9. These data gave immediate evidence that the specific binding of target and split aptamer fragments activated palindromic fragment-mediated BERA process.

3.4. Optimization of experimental conditions

In order to achieve the optimal analytical performance, a series of key experimental parameters including the concentration of MB, the amounts of UDG, and the reaction temperature and time for ERA were optimized (Fig. 3). The MB probe can not only serve as recognition element, primer, and polymerization template for BERA reaction but also the tracer for fluorescence signal output. So we investigated the variance of the $(F-F_0)/F_0$ value with different concentrations of MB, where F and F_0 were the fluorescence emission peak intensity at 519 nm in the presence and absence of ATP, respectively. As shown in Fig. 3A, the $(F-F_0)/F_0$ value continuously increased with increasing of MB concentration and reached equilibrium when the concentration was 5 μM. So, 5 μM was chosen as the optimal concentration in the subsequent research. Moreover, the amplifying efficiency of this strategy was also greatly depended on the amounts of UDG, thus we optimized the concentration of UDG on the basis of the fluorescence signal intensity in the presence and absence of 5.0×10^5 pM ATP. As we can see from Fig. 3B, for the positive sample, the fluorescence intensity was gradually intensified with increasing of the concentration of UDG and experienced almost no change when the concentration reached 1 U μL^{-1} (curve a), while there was no obvious change for the blank sample (curve b). Thereby, 1 U μL^{-1} was chosen as the optimized concentration in the following experiments. Furthermore, the reaction temperature is also crucial in our assay. It was found from Fig. 3C that the fluorescence signal intensity enhanced upon an increase of

Table 3
ATP analysis in real samples.

Spiked amount (pM)	Measured (pM)		Recovery (%) ± SD	
	Our method	HPLC	Our method	HPLC
1×10^1	$(1.017 \pm 0.026) \times 10^1$	$(0.972 \pm 0.017) \times 10^1$	101.7 ± 2.9	97.2 ± 1.7
1×10^2	$(0.986 \pm 0.027) \times 10^2$	$(0.963 \pm 0.047) \times 10^2$	98.6 ± 2.7	96.3 ± 4.7
1×10^3	$(0.979 \pm 0.041) \times 10^3$	$(1.015 \pm 0.028) \times 10^3$	97.9 ± 4.1	101.5 ± 2.8

the reaction temperature and reached a plateau at 50 °C (curve a), nevertheless, there was no obvious change for that of the blank sample (curve b). Hence, 50 °C was chosen as the optimum reaction temperature. Additionally, the reaction time of the sensing strategy was optimized, and the results were shown in Fig. 3D. We observed the fluorescence signal intensity for the positive sample increased with the increase of the reaction time and reached the maximum value at 90 min, however, there was no obvious change for that of the blank sample. The highest signal-to-noise (S/N) was obtained when the reaction time was 90 min. Therefore, 90 min was adopted as the optimal reaction time in the following research.

3.5. Analytical performance of the biosensor for ATP detection

Under the optimized conditions, the analytical performance of the present biosensor was investigated towards the detection of ATP with different concentrations. Fig. 4A depicted the fluorescence signal of this biosensor in responses to different concentrations of ATP. It was observed that the signal intensities at 519 nm increased significantly with the increasing concentration of ATP from 0 to 5.0×10^5 pM. The plot of the fluorescence signal intensity versus the logarithm value of ATP concentrations displayed a good linear dependence in the range from 1 pM to 500 nM (Fig. 4B). The linear regression equation was $F = 0.187 + 156.267 \times \lg (C_{ATP}/pM)$ with a correlation coefficient of 0.996. The detection limit was calculated to be 0.81 pM in terms of the rule of 3 times standard deviation over the blank response. Additionally, the analytical performance of our biosensor in the quantitative assay of ATP was compared with that of the previous reported methods, and the results were shown in Table 2. It was found that the sensitivity of this strategy was superior to the majority of the existing methods for ATP assay. What is more, our constructed fluorescence sensing strategy allowed to *rapid*, simple, convenient, one-step homogenous detection of ATP with ultrahigh specificity.

3.6. Specificity study

The specificity of the proposed strategy was evaluated by challenging the system with target ATP and other non-target molecules including GTP, CTP, and UTP, and the results were shown in Fig. 5. As expected, a remarkably strong fluorescence response was observed in the presence of ATP, while there was no significant change in the fluorescence intensity in the detection of 500 nM GTP, 500 nM CTP, and 500 nM UTP in comparison with the blank test. Moreover, the mixture containing 500 nM GTP, 500 nM CTP, 500 nM UTP, and 500 nM ATP did not lead to a significant signal change compared with the case of solely ATP. These results manifested the excellent specificity of the proposed fluorescence biosensor for ATP detection.

3.7. Real sample analysis

To evaluate the applicability of our biosensor in complicated biological environment, the quantitative assay of ATP in human serum samples was studied. A serious of ATP standard solutions at 0, 10 pM, 100 pM, and 1 nM were separately spiked into the human serum samples and measured directly. As illustrated in Fig. 6, the fluorescence signals detected in the human serum were in good agreement with those obtained in buffer, and the discrepancies between the two samples were extremely small. It is indicated that the ATP assay can be carried out in complex biological matrix with this sensing strategy. To further validate the universality of this strategy, high performance liquid chromatography (HPLC) was also used for the detection of the serum samples. As shown in Table 3, the data obtained by our method had no obvious discrepancies compared to those obtained via HPLC, and the discrepancies between the two methods were all smaller than 4.5%. In addition, the recovery of the proposed approach was in the range of 93.8%–104.6%. This clearly indicated that the method we proposed might hold great promise for real sample analysis with excellent reliability and accuracy. In order to further investigate the applicability of this constructed biosensor in real samples, the quantitative assay of ATP in HeLa cells were studied (Fig. S1). It was observed that the fluorescence intensities gradually increased with increasing of the numbers of HeLa cells. The above results clearly revealed our strategy can be applied for quantitative assay of ATP in cell extracts.

4. Conclusions

In summary, we report the development of a facile and robust fluorescence sensing strategy for ultrasensitive and highly specific detection of ATP. This strategy relies on proximity binding-triggered the release of palindromic sequence that initiates bidirectional enzymatic repairing amplification reaction. Thus, amplified detection of target can be achieved due to the combination of proximity ligation assay with BERA. As we know, it is the first time that fluorescence signal amplification was realized by palindromic fragment-mediated BERA for the detection of ATP. On the basis of the amplification strategy, our biosensor exhibits high sensitivity with an excellent detection limit as low as 0.81 pM, which is better than most of the existing methods. And it offers the merits of ultrahigh specificity, shortened analysis time, and simplified operation. Additionally, the proposed strategy holds the potential of being extended for the detection of other targets by redesigning the corresponding binding molecules. Therefore, the proximity-enabled BERA strategy indeed creates a versatile sensing platform for the detection of ATP and related disease diagnosis and biomedical research.

Declaration of competing interest

The authors declare that they have no known competing financial interests or personal relationships that could have appeared to influence the work reported in this paper.

CRediT authorship contribution statement

Shasha Li: Conceptualization, Methodology, Software, Investigation, Writing - original draft. **Su Liu:** Validation, Formal analysis, Visualization, Software. **Jingfeng Wang:** Resources, Software, Investigation. **Yihan Zhao:** Resources, Software, Investigation. **Rufeng Zhang:** Resources, Software, Investigation. **Xiaonan Qu:** Resources, Software, Investigation. **Yu Wang:** Writing - review & editing, Formal analysis, Supervision, Data curation. **Jiadong Huang:** Supervision, Data curation, Project administration. **Jinghua Yu:** Funding acquisition, Project administration.

Acknowledgements

This work was supported by National Natural Science Foundation of China (31471644), the Primary Research & Development Plan of Shandong Province (2017GSF220009), and the program for Taishan Scholer of Shandong provinces (ts201712048).

Appendix A. Supplementary data

Supplementary data to this article can be found online at https://doi.org/10.1016/j.aca.2020.01.006.

References

[1] C.H. Zhang, H. Wang, J.W. Liu, Amplified split aptamer sensor delivered using block copolymer nanoparticles for small molecule imaging in living cells, ACS Sens. 3 (2018) 2526–2531.

[2] J. Deng, K. Wang, M. Wang, P. Yu, L. Mao, Mitochondria targeted nanoscale zeolitic imidazole framework-90 for ATP imaging in live cells, J. Am. Chem. Soc. 139 (2017) 5877–5882.

[3] Z. Xu, T. Zhang, Y. Gu, F. Liu, H. Liu, N. Lu, et al., New strategy for ultrasensitive aptasensor fabrication: D-A-D constitution as a charge transfer platform and recognition element, ACS Appl. Mater. Interfaces 11 (2019) 17894–17901.

[4] Y. Guo, X. Sun, G. Yang, J. Liu, Ultrasensitive detection of ATP based on ATP regeneration amplification and its application in cell homogenate and human serum, Chem. Commun. 50 (2014) 7659–7662.

[5] Y. Guo, J. Liu, G. Yang, X. Sun, H.Y. Chen, J.J. Xu, Multiple turnovers of DNAzyme for amplified detection of ATP and reduced thiol in cell homogenates, Chem. Commun. 51 (2015) 862–865.

[6] X.M. Hai, N. Li, K. Wang, Z.Q. Zhang, J. Zhang, F.Q. Dang, A fluorescence aptasensor based on two-dimensional sheet metal-organic frameworks for monitoring adenosine triphosphate, Anal. Chim. Acta 998 (2018) 60–66.

[7] Y.S. Guo, S. Li, J. Liu, G.X. Yang, Z.M. Sun, J. Wan, Double functional aptamer switch probes based on gold nanorods for intracellular ATP detection and targeted drugs transportation, Sens. Actuators B Chem. 235 (2016) 655–662.

[8] J. Yuan, Z. Deng, H. Liu, X. Li, J. Li, Y. He, et al., Cell-surface-anchored ratiometric DNA nanoswitch for extracellular ATP imaging, ACS Sens. 4 (2019) 1648–1653.

[9] Y. Wang, X. Shang, J. Liu, Y. Guo, ATP mediated rolling circle amplification and opening DNA-gate for drug delivery to cell, Talanta 176 (2018) 652–658.

[10] F. Liu, Y. Guo, Y. Hu, X. Zhang, X. Zheng, Intracellular dark-field imaging of ATP and photothermal therapy using a colorimetric assay based on gold nanoparticle aggregation via tetrazine/trans-cyclooctene cycloaddition, Anal. Bioanal. Chem. 411 (2019) 5845–5854.

[11] C. Lin, Y. Chen, Z. Cai, Z. Zhu, Y. Jiang, C.J. Yang, et al., A label-free fluorescence strategy for sensitive detection of ATP based on the ligation-triggered supersandwich, Biosens. Bioelectron. 63 (2015) 562–565.

[12] T.T. Zhang, Z.Q. Xu, H.X. Xu, Y. Gu, Y. Xing, X.Y. Yan, H. Liu, N.N. Lu, Y. Song, S.Y. Zhang, Z.Q. Zhang, M. Yang, Catechol and zwitterion-bifunctionalized poly(ethylene glycol) based ultrasensitive antifouling electrochemical aptasensor for the quantification of adenosine triphosphate in biological media, Sens. Actuators B Chem. 288 (2019) 469–475.

[13] Y.P. Dong, Y. Zhou, J. Wang, J.J. Zhu, Electrogenerated chemiluminescence resonance energy transfer between Ru(bpy)3(2+) electrogenerated chemiluminescence and gold nanoparticles/graphene oxide nanocomposites with graphene oxide as coreactant and its sensing application, Anal. Chem. 88 (2016) 5469–5475.

[14] X.M. Hai, N. Li, K. Wang, Z.Q. Zhang, J. Zhang, F.Q. Dang, A fluorescence aptasensor based on two-dimensional sheet metal-organic frameworks for monitoring adenosine triphosphate, Anal. Chim. Acta 998 (2018) 60–66.

[15] H. Fang, H.J. Yin, M.Y. Lv, H.J. Xu, Y.M. Zhao, X. Zhang, et al., Approach for determination of ATP:ADP molar ratio in mixed solution by surface-enhanced Raman scattering, Biosens. Bioelectron. 69 (2015) 71–76.

[16] L. Kashefi-Kheyrabadi, M.A. Mehrgardi, Aptamer-conjugated silver nanoparticles for electrochemical detection of adenosine triphosphate, Biosens. Bioelectron. 37 (2012) 94–98.

[17] C. Li, M. Numata, M. Takeuchi, S. Shinkai, A sensitive colorimetric and fluorescent probe based on a polythiophene derivative for the detection of ATP, Angew. Chem. Int. Ed. 44 (2005) 6371–6374.

[18] X. Zhang, Z. Yang, Y. Chang, M. Qing, R. Yuan, Novel 2D-DNA-nanoprobe-mediated enzyme-free-target-recycling amplification for the ultrasensitive electrochemical detection of MicroRNA, Anal. Chem. 90 (2018) 9538–9544.

[19] J. Yang, B. Dou, R. Yuan, Aptamer/protein proximity binding-triggered molecular machine for amplified electrochemical sensing of thrombin, Anal. Chem. 89 (2017) 5138–5143.

[20] N. Li, L. Liu, M.H. Xiang, J.W. Liu, R.Q. Yu, J.H. Jiang, Proximity-induced hybridization chain assembly with small-molecule linked DNA for single-step amplified detection of antibodies, Chem. Commun. 55 (2019) 4387–4390.

[21] X. Chang, C. Zhang, Construction of a multiple-aptamer-based DNA logic device on live cell membranes via associative toehold activation for accurate cancer cell identification, Chem. Commun. 141 (2019) 12738–12743.

[22] L. Wang, W. Li, J. Sun, S.Y. Zhang, S. Yang, J. Li, Imaging of receptor dimers in zebrafish and living cells via aptamer recognition and proximity-induced hybridization chain reaction, Anal. Chem. 90 (2018) 14433–14438.

[23] H. Gao, X. Wang, M. Li, H. Qi, Q. Gao, C. Zhang, Proximity hybridization-regulated electrogenerated chemiluminescence bioassay of alpha-fetoprotein via target-induced quenching mechanism, Biosens. Bioelectron. 98 (2017) 62–67.

[24] J. Zhu, H. Gan, J. Wu, Molecular machine powered surface programmatic chain reaction for highly sensitive electrochemical detection of protein, Anal. Chem. 90 (2018) 5503–5508.

[25] M. Zou, D. Li, R. Yuan, Y. Xiang, Metal-ion dependent DNAzyme recycling amplification for sensitive and homogeneous immuno-proximity binding assay of alpha-fetoprotein biomarker, Biosens. Bioelectron. 92 (2017) 624–629.

[26] J. Yang, B. Dou, R. Yuan, Y. Xiang, Proximity binding and metal ion-dependent DNAzyme cyclic amplification-integrated aptasensor for label-free and sensitive electrochemical detection of thrombin, Anal. Chem. 88 (2016) 8218–8223.

[27] Y.S. Ang, J.J. Li, P.J. Chua, C.T. Ng, B.H. Bay, L.L. Yung, Localized visualization and autonomous detection of cell surface receptor clusters using DNA proximity circuit, Anal. Chem. 90 (2018) 6193–6198.

[28] C. Zong, J. Wu, M. Liu, L. Yang, L. Liu, F. Yan, et al., Proximity hybridization-triggered signal switch for homogeneous chemiluminescent bioanalysis, Anal. Chem. 86 (2014) 5573–5578.

[29] X.Q. Leng, Y. Wang, S. Liu, Q.Q. Pei, X.J. Cui, Y.Q. Tu, X.J. Liu, J.D. Huang, Enzymatic repairing amplification-based versatile signal-on fluorescence sensing platform for detecting pathogenic bacteria, Sens. Actuators B Chem. 252 (2017) 689–696.

[30] L.J. Wang, Z.Y. Wang, Q.Y. Zhang, B. Tang, C.Y. Zhang, Cyclic enzymatic repairing-mediated dual-signal amplification for real-time monitoring of thymine DNA glycosylase, Chem. Commun. 53 (2017) 3878–3881.

[31] M.J. Stern, G.F. Ames, N.H. Smith, E.C. Robinson, C.F. Higgins, Repetitive extragenic palindromic sequences: a major component of the bacterial genome, Cell 37 (1984) 1015–1026.

[32] R. Zeng, Z. Luo, L. Zhang, D. Tang, Platinum nanozyme-catalyzed gas generation for pressure-based bioassay using polyaniline nanowires-functionalized graphene oxide framework, Anal. Chem. 90 (2018) 12299–12306.

[33] F. Li, H. Zhao, Z.Y. Wang, Z.S. Wu, Z. Yang, C.C. Li, et al., Single palindromic molecular beacon-based amplification for genetic analysis of cancers, Biosens. Bioelectron. 91 (2017) 692–698.

[34] R. Zeng, Z. Luo, L. Su, L. Zhang, D. Tang, Palindromic molecular beacon based Z-scheme BiOCl-Au-CdS photoelectrochemical biodetection, Anal. Chem. 91 (2019) 2447–2454.

[35] Z.F. Shen, F. Li, Palindromic molecule beacon-based cascade amplification for colorimetric detection of cancer genes, Anal. Chem. 90 (2018) 3335–3340.

[36] C.H. Zhang, Y. Tang, Y.Y. Sheng, H. Wang, Z. Wu, J.H. Jiang, Ultrasensitive detection of microRNAs using catalytic hairpin assembly coupled with enzymatic repairing amplification, Chem. Commun. 52 (2016) 13584–13587.

[37] H. Jang, C.Y. Lee, S. Lee, K.S. Park, H.G. Park, Flap endonuclease-initiated enzymatic repairing amplification for ultrasensitive detection of target nucleic acids, Nanoscale 11 (2019) 3633–3638.

[38] D.M. Zhou, W.F. Du, Q. Xi, J. Ge, J.H. Jiang, Isothermal nucleic acid amplification strategy by cyclic enzymatic repairing for highly sensitive microRNA detection, Anal. Chem. 86 (2014) 6763–6767.

[39] Y. Wei, Y. Chen, H. Li, S. Shuang, C. Dong, G. Wang, An exonuclease I-based label-free fluorometric aptasensor for adenosine triphosphate (ATP) detection with a wide concentration range, Biosens. Bioelectron. 63 (2015) 311–316.

[40] S. Liu, Y. Wang, C. Zhang, Y. Lin, F. Li, Homogeneous electrochemical aptamer-based ATP assay with signal amplification by exonuclease III assisted target recycling, Chem. Commun. 49 (2013) 2335–2337.

[41] Y. Song, X. Yang, Z. Li, Y. Zhao, A. Fan, Label-free chemiluminescent ATP aptasensor based on graphene oxide and an instantaneous derivatization of guanine bases, Biosens. Bioelectron. 51 (2014) 232–237.

[42] M. Li, J. Zhang, S. Suri, L.J. Sooter, D. Ma, N. Wu, Detection of adenosine triphosphate with an aptamer biosensor based on surface-enhanced Raman scattering, Anal. Chem. 84 (2012) 2837–2842.

[43] Q. Song, R. Wang, F. Sun, H. Chen, Z. Wang, N. Na, et al., A nuclease-assisted label-free aptasensor for fluorescence turn-on detection of ATP based on the in situ formation of copper nanoparticles, Biosens. Bioelectron. 87 (2017) 760–763.

[44] T. Zhao, C. Lin, Q. Yao, X. Chen, A label-free electrochemiluminescent sensor for ATP detection based on ATP-dependent ligation, Talanta 154 (2016) 492–497.